



<b>Publication Year</b>	2019
<b>Acceptance in OA@INAF</b>	2021-01-07T15:24:19Z
<b>Title</b>	High precision mapping of single-pixel Silicon Drift Detector for applications in astrophysics and advanced light source
<b>Authors</b>	Cirrinzione, D.; Ahangarianabhari, M.; AMBROSINO, Filippo; Bajnati, I.; Bellutti, P.; et al.
<b>DOI</b>	10.1016/j.nima.2018.10.114
<b>Handle</b>	<a href="http://hdl.handle.net/20.500.12386/29563">http://hdl.handle.net/20.500.12386/29563</a>
<b>Journal</b>	NUCLEAR INSTRUMENTS & METHODS IN PHYSICS RESEARCH. SECTION A, ACCELERATORS, SPECTROMETERS, DETECTORS AND ASSOCIATED EQUIPMENT
<b>Number</b>	936

---

1 NIMA POST-PROCESS BANNER TO BE  
2 REMOVED AFTER FINAL ACCEPTANCE

---

3 High precision mapping of single-pixel Silicon Drift  
4 Detector for applications in astrophysics and advanced  
5 light source

6 D. Cirrincione<sup>a,b,\*</sup>, M. Ahangarianabhari<sup>c,d</sup>, F. Ambrosino<sup>e</sup>, I. Bajnati<sup>f,e</sup>,  
7 P. Bellutti<sup>g,h</sup>, G. Bertuccio<sup>c,d</sup>, G. Borghi<sup>g,h</sup>, J. Bufon<sup>i,a</sup>, G. Cautero<sup>i,a</sup>,  
8 F. Ceraudo<sup>f,e</sup>, Y. Evangelista<sup>e,j</sup>, S. Fabiani<sup>e,j</sup>, M. Feroci<sup>e,j</sup>, F. Ficorella<sup>g,h</sup>,  
9 M. Gandola<sup>c,d</sup>, F. Mele<sup>c,d</sup>, G. Orzan<sup>a</sup>, A. Picciotto<sup>g,h</sup>, M. Sammartini<sup>c,d</sup>,  
10 A. Rachevski<sup>a</sup>, I. Rashevskaya<sup>h</sup>, S. Schillani<sup>i,a</sup>, G. Zampa<sup>a</sup>, N. Zampa<sup>a</sup>,  
11 N. Zorzi<sup>g,h</sup>, A. Vacchi<sup>a,b</sup>

12 <sup>a</sup>*INFN Trieste, Trieste, Italy*

13 <sup>b</sup>*Dipartimento di Matematica ed Informatica, Università Udine, Udine, Italy*

14 <sup>c</sup>*Politecnico di Milano, Como, Italy*

15 <sup>d</sup>*INFN Milano, Milan, Italy*

16 <sup>e</sup>*INAF-IAPS, Rome, Italy*

17 <sup>f</sup>*CEA Saclay, Paris, France*

18 <sup>g</sup>*Fondazione Bruno Kessler, Trento, Italy*

19 <sup>h</sup>*TIFPA INFN, Trento, Italy*

20 <sup>i</sup>*Elettra-Sincrotrone Trieste S.C.p.A., Trieste, Italy*

21 <sup>j</sup>*INFN Roma Tor Vergata, Rome, Italy*

---

22 **Abstract**

23 A Silicon Drift Detector with 3x3 mm<sup>2</sup> sensitive area was designed by INFN  
24 of Trieste and built by FBK-Trento. It represents a single-pixel precursor of a  
25 monolithic matrix of multipixel Silicon Drift Detectors and, at the same time,  
26 a model of one cell Fluorescence Detector System (XAFS) for SESAME.  
27 The point-by-point mapping tests of the detector were carried out in the X-ray  
28 facilities at INAF-IAPS in Rome, equipped with a motorized two-axis micro-

---

\*Corresponding author  
Preprint submitted to Elsevier.  
Email address: Daniela.Cirrincione@ts.infn.it (D. Cirrincione)

29 metric positioning system. High precision characterization of this detector was  
30 done with a radioactive  $^{55}\text{Fe}$  source and a collimated Ti X-ray tube equipped  
31 with a Bragg crystal monochromator.

32 The mapping in different positions and bias condition was specifically-aimed  
33 to the detailed analysis of the charge collection efficiency at the edge of the  
34 detector. The result is important to understand and verify the aspects related  
35 to the collection of the signal with respect to the position of interactions of  
36 the photons, especially in consideration of the new design and development of  
37 monolithic multipixel detectors.

38 *Keywords:* Silicon Drift Detectors, SDD, mapping

39 *PACS:* 29.30.Kv, 29.40.Wk, 07.85.Qe

---

## 40 **1. Detector and experimental setup**

41 The detector mapped is a single-pixel Silicon Drift Detector (SDD), with  
42  $3.0 \times 3.0 \text{ mm}^2$  [Fig.1] sensitive area, designed by INFN of Trieste and built by  
43 FBK-Trento. The SDD has an entrance window (with bias voltages  $V_{\text{WIN}}$ ) in  
44 the front side and, in the backside, the drift cathodes (bias voltage  $V_{\text{OR}}$  and  
45  $V_{\text{IR}}$  is applied respectively to the outer and inner drift cathodes) and the central  
46 small anode, connected with the readout by the ultra-low noise SIRIO [1] charge  
47 sensitive preamplifier. The potential energy of the electrons in the SDD has the  
48 shape of a funnel [1].

49 The detector mapping [2, 3] were carried out in the X-ray facilities at INAF-  
50 IAPS in Rome, equipped with a motorized two-axis micrometric positioning sys-  
51 tem, a radioactive  $^{55}\text{Fe}$  source and a collimated Ti X-ray tube with a Bragg crys-  
52 tal monochromator. The measurements were carried out in an air-conditioned  
53 room with an ambient temperature of  $18 \text{ }^\circ\text{C}$ .

## 54 **2. Measurements**

55 Before performing the mapping, it is important to determine the dimension  
56 of the beam which has a oblong gaussian shape (for the X axis the FWHM of

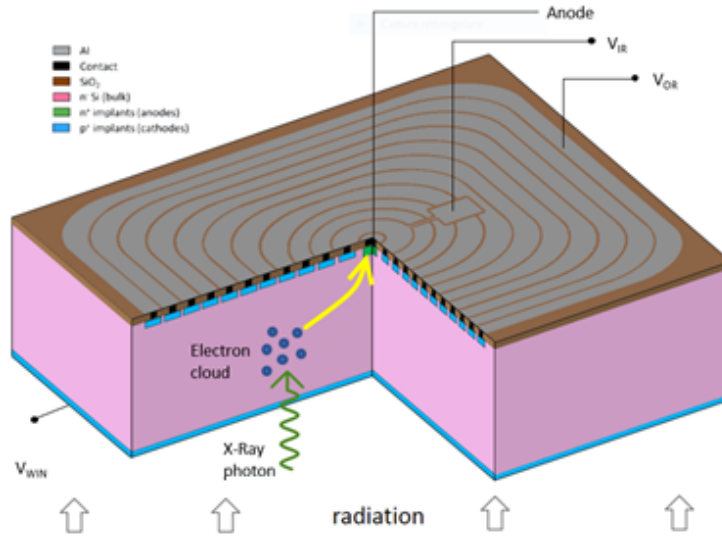


Figure 1: Working principle and structure of the detector.

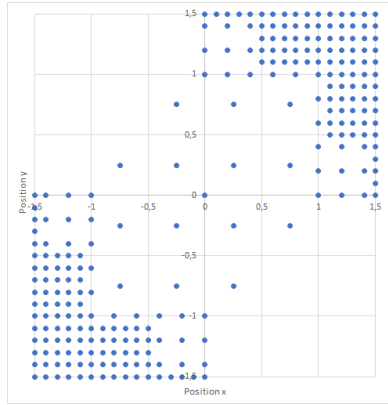
57 the beam is  $165.48 \mu\text{m}$  and for the Y axis is  $128.83 \mu\text{m}$ ), to reveal the center  
 58 position of the SDD, to align the detector with the X-Ray tube, and to calibrate  
 59 the system with the radioactive  $^{55}\text{Fe}$  source and Ti X-ray tube.

60 For the point-by-point mapping, we have used the collimated Ti X-ray tube  
 61 and we have acquired data at coarse steps in the central zone ( $500 \mu\text{m}$ ) and at  
 62 finer steps ( $100 \mu\text{m}$ ) near the edges of the detector. The measurements have  
 63 been made for 4 different outer ring voltages. [Fig.2]

### 64 3. Results and conclusions

65 The outer ring voltage changes the efficient area of the detector. This detec-  
 66 tor has a larger effective area ( $2.7 \times 2.7 \text{ mm}^2$ ) [Fig.3 and Fig.4] than the previous  
 67 version tested in 2016 ( $2.5 \times 2.5 \text{ mm}^2$ ) [3], but still less than the nominal  $3.0 \times 3.0$   
 68  $\text{mm}^2$  area.

69 The mapping allows to verify aspects related to the charge collection to  
 70 the detector's edge. Furthermore, the mapping allows the cross check of the  
 71 device simulation and fosters the progress in the design and development of



Outer ring voltage ( $V_{OR}$ )	Windows voltage ( $V_{WIN}$ )	Inner ring voltage ( $V_{IR}$ )
-144.6 V	-85.10 V	-23.8 V
-124.4 V	-80.66 V	-21.13 V
-104.06 V	-80.85 V	-19.81 V
-84.1 V	-80.97 V	-18.59 V

Figure 2: Scheme of the map used for the acquisitions with different steps for the central region and the edge of the detector, and table showing the four different bias conditions used for the measurements.

72 new monolithic matrix of multipixel Silicon Drift Detectors for applications in  
73 astrophysics and advanced light source.

#### 74 Acknowledgments

75 This work has been made within the ReDSOX-2 INFN research project, sup-  
76 ported with the contribution of the Italian Ministry of University and Research  
77 within the EUROFEL Project and FBK-INFN agreement 2015-03-06.

#### 78 References

- 79 [1] G. Bertuccio, et al., X-Ray Silicon Drift Detector CMOS Front-End System  
80 with High Energy Resolution at Room Temperature, IEEE Transactions  
81 on Nuclear Science 63.1 (2016), pp. 400-406.
- 82 [2] A. Castoldi, et al., 2-D mapping of the response of SDD cells of different  
83 shape in monolithic arrays for XRF spectroscopy. Nuclear Science Symposi-  
84 um, Medical Imaging Conference and Room-Temperature Semiconductor  
85 Detector Workshop (NSS/MIC/RTSD), IEEE (2016), pp. 1-3.

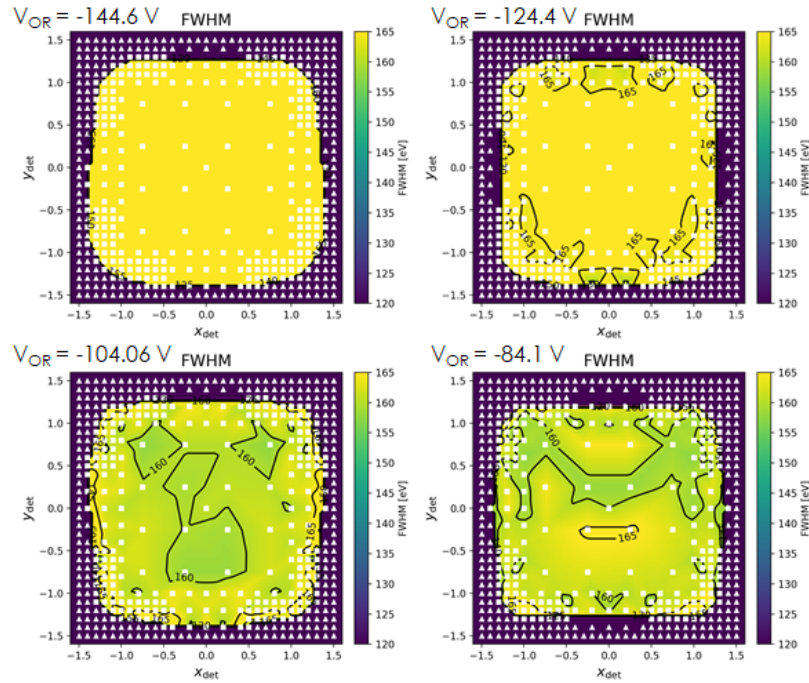


Figure 3: FWHM maps. Squares represent the points having more than 25 counts for the Ti  $K\alpha$  line, which were processed. Triangles correspond to measurements having less than 25 counts for the Ti  $K\alpha$  line and were discarded. In order to have a better view of the results, the points acquired are mirrored to represent all the detector area. Values between the experimental points were obtained through linear interpolation.

- 86 [3] F. Ceraudo, Development of space instrumentation for high throughput X-  
 87 ray Astronomy, Master Degree Thesis, University of Roma Sapienza (AA  
 88 2015/16).

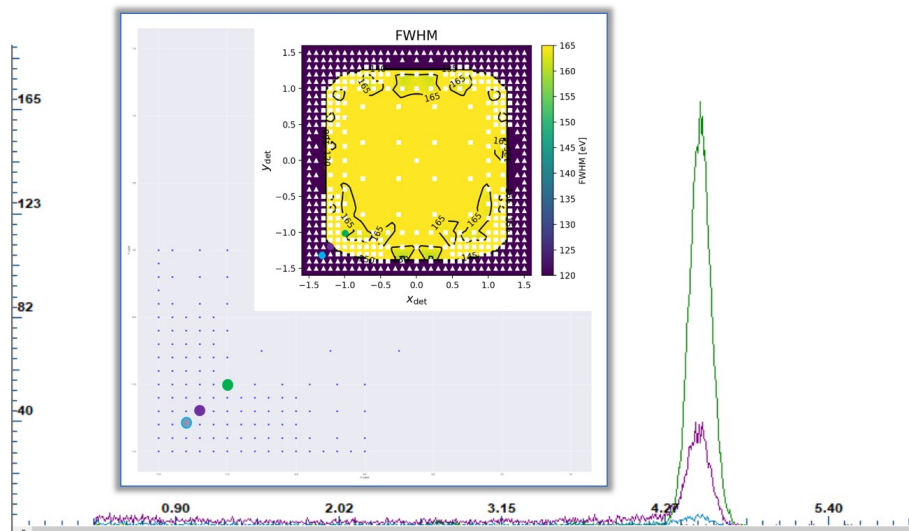


Figure 4: Spectra (Ti  $K\alpha$  line) at points: green (-1.0;-1.0), purple (-1.2;-1.2) and blue (-1.3;-1.3) with  $VOR = -124.4$  V. The centroid of the peak is, respectively, at 4.51, 4.50 and 4.47 keV, the mismatch is due to the progressive growth of the left shoulder of the peak caused by truncated events where a part of the signal charge is lost to the periphery of the detector.